

Technological Challenges in Low-mass Interstellar Probe Communication

David G. Messerschmitt

Roger Strauch Emeritus Professor, Dept. of EECS, University of California at Berkeley, USA

Philip Lubin

Professor, Dept. of Physics, University of California at Santa Barbara, USA

Ian Morrison

Research Fellow, International Centre for Radio Astronomy Research, Curtin University, Australia

Building on a preliminary paper design of a downlink from a swarm of low-mass interstellar probes for returning scientific data from the vicinity of Proxima Centauri, the most critical technology issues are summarized, and their significance is explained in the context of the overall system design. The primary goal is to identify major challenges or showstoppers if such a downlink were to be constructed using currently available off-the-shelf technology, and thereby provide direction and motivation to future research on the constituent design challenges and technologies. While there are not any fundamental physical limits that prevent such communication systems, currently available technologies fall significantly short in several areas and there are other major design challenges with uncertain solutions. The greatest identified challenges are in mass constraints, multiplexing simultaneous communication from multiple probes to the same target exoplanet, attitude control and pointing accuracy, and Doppler shifts due to uncertainty in probe velocity. The greatest technology challenges are electrical power, high power and wavelength-agile optical sources, very selective and wavelength-agile banks of optical bandpass filters, and single-photon detectors with extremely low dark-count rates. For a critical subset of these, we describe the nature of the difficulties we encounter and their origins in the overall system context. A receiver that limits reception to a single probe is also considered and compared to the swarm case.

I. Introduction

A near-term opportunity for exploration of nearby stars is low-mass probes accelerated to relativistic speeds using a directed energy (DE) driven sail for propulsion [1], [2]. Such a mission is worthwhile only if acquired scientific data can be returned to earth using a communication downlink [3]. In a companion paper [4] we have performed a paper design and idealized theoretical evaluation of the feasibility of such a data downlink. Although we are not aware of any fundamental physical limits on the data rate at which scientific data can be reliably recovered, serious challenges arise when relating the requirements to resource limits (such as probe mass and electrical power) and available technologies (such as sources, detectors, and filters). Current technologies fall considerably short of minimum requirements in several areas, and the feasibility of a downlink is dependent on enabling technology advances driven either by the natural advancement in technology or specific technology developed in the course of R&D dedicated to this application. These enabling technologies are needed between now and the first launch (for transmitter) or coinciding with the arrival of the first scientific data (for the receiver). The primary goal of this evaluation was thus to identify the most critical technological shortcomings that present an obstacle to a successful mission, and thus help to guide future R&D efforts addressing these shortcomings. Here we summarize those critical technologies, emphasizing their role within the overall downlink system based on the results from [4]. This paper is based on [5], updating and adding some material.

II. Nominal design

A simplified block schematic of the optical signal path is shown in Fig.1 as a basis for later discussion. It illustrates the primary elements of that signal path discussed in this paper and how they relate to one another. A model of the downlink has a number of configuration parameters and performance metrics. A *nominal* design invokes compatible

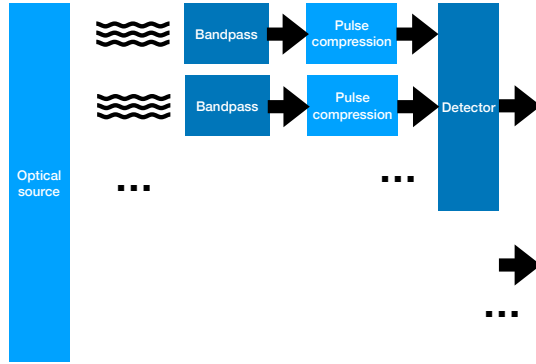


Fig. 1 The important elements in the optical signal path from electrical power input to photon detection events at the output. The optical source generates pulses of optical power which propagate to the receiver, where a bandpass filter limits noise and interference and (possibly) separates signals from different probes. The pulse compression is a phase-only filter that concentrates signal pulses in time, moderating the peak power required at the optical source. The optical detector labels individual photon detection events with time stamps. Each detector may be shared over multiple receive apertures and will be replicated many times for different sets of apertures.

(and hopefully reasonable) choices for the parameters listed in Tbl.1. A model of the downlink, including both physical layer (having to do with physical elements and propagation) and transport layer (having to do with modulation and coding), yields a set of performance metrics listed in Tbl.2. The model is idealized, ignoring many practicalities such as pointing inaccuracy, aperture sidelobes, and coding shortfalls, and thus yields optimistic values for all the metrics.*

The probe mass is assumed to be γ grams, where $\gamma \geq 1$ is the *mass ratio*. For a fixed launch infrastructure, increasing γ , while reducing u_0 , also increases \mathcal{R}_0 due to larger transmit aperture and electrical power. An optimum choice of γ minimizes the total *data latency* (time elapsed from launch to completion of scientific data download) for a given *data volume* (total number of bits or bytes downloaded and recovered reliably). For a particular set of scaling laws, we find that transmission should be terminated after the probe reaches a distance of approximately $1.10 \cdot D_0$, with a resulting nominal transmission time of 2.12 yr.

The signal-to-background ratio SBR is the ratio of average signal photon rate to average background radiation photon rate for all sources of background including unresolved sources of noise (Zodiacal radiation, deep star field, and scattered moonlight), a point source of interference radiation from the nearby target star, dark counts in the received optics and the optical detector, and incomplete extinguishment of the optical source during “off” periods. With the notable exception of dark counts, the noise and interference power is limited by a narrow optical bandpass filter with bandwidth $W_e = 10$ MHz before it contributes to SBR. We anticipate using superconducting optical detectors shared over multiple apertures in order to achieve the very low dark count rate Λ_D^S (see §III.D). The chosen objective for SBR is sufficiently large that theoretical limits indicate minimal impact on the data rate at which reliable detection can be achieved. During nighttime we found that scattered moonlight and dark counts are the most significant sources of background radiation for typical interference parameters.

Theoretical limits also indicate that reliable data recovery can be achieved by constructing a signal at the detector composed of narrow pulses of duration T_s , with the average number of photons detected K_s within each pulse. The small value $K_s = 0.2$ (termed photon starvation mode) is advantageous in minimizing peak transmit power, but it indicates that a random $\sim 80\%$ of the pulses are unobservable by the receiver because zero photons are detected. Reliable extraction of scientific data is achieved by error-correction coding (ECC), which adds substantial redundancy to the scientific data before transmission. In the nominal design, 17% of the total transmitted data is scientific and 83% is redundant information used for error control and to counter random outages. This design approach has been validated in bench testing [7].

Scattered sunlight during the daytime is far too large to overcome, and thus daylight as well as adverse weather events

* See [4] for plots of changes in metrics as parameters are varied one at a time. Software code allowing the reader to substitute their own model parameters and calculate the resulting metrics is available at [6].

Table 1 Design parameters and values for a nominal design including reception from a single probe and simultaneous reception from a swarm of probes.

Parameter	Description	Units	Swarm	Single
\mathcal{R}_0	Data rate, before outages, immediately following encounter	bits/s	1.	
D_0	Distance to target star (Proxima Centauri)	ly	4.24	
u_0	Speed of probe as fraction of speed of light c		0.2	
λ_0	Receive wavelength	nm	400	
A_e^T	Effective area of transmit aperture	cm ²	100.	
Ω_A	Solid angle of receive collector coverage	arcsec ²	10.	0.01
SBR	Signal-to-background-radiation ratio at each aperture and for the receive collector as a whole		4.0	
Λ_D^S	Average rate of dark counts referenced to each aperture	ph/yr	32.	
δ	Duty cycle for burst-mode transmission		1.9×10^{-4}	
T_s	Individual pulse width at optical detector	ns	100.	
K_s	Average number of photon detections in each pulse		0.2	
W_e	Effective optical bandwidth ($W_e T_s = 1$)	MHz	10.	
P_0	Outage probability (daylight and clouds)		0.57	

are treated as a receiver-initiated outage. The total outage probability P_0 in Tbl.1 assumes a daylight outage probability (averaged over a year) of 52% and a weather outage probability of 10%. Through a combination of interleaving and ECC, a post-outage data rate approaching $\mathcal{R}_a = \mathcal{R}_0 \cdot (1 - P_0)$ (nominally 0.43 bits/s with reliable recovery of scientific data) can be achieved, and significantly the probe need not have knowledge of outage conditions.

Dark counts are perverse photon-detection events unrelated to incident signal, noise, and interference, and may occur in the optics and photonics (due to blackbody radiation) as well as optical detectors [8]. Although it is clear that superconducting optical detectors are required, and they fortunately have no intrinsic mechanism for dark counts, nevertheless occasional detector dark counts will be caused by non-idealities such as impurities and radiation. Since the achievable dark count rate Λ_D is largely technology driven, there is no solid rationale for choosing a specific numerical value. The nominal value in Tbl.1 is chosen to render the dark-count contribution to background radiation equal to that of scattered moonlight (for a full moon) within the context of the other design parameters. Moonlight and dark counts are then the two dominant sources of background radiation in equal measure.

III. Receiver issues

The technology issues that arise in the receiver can only be addressed in the context of the receive collector architecture, so that is briefly described before addressing the optical processing and detector technology challenges.

A. Coverage

Communications is much easier for a single probe heading to a single target but we also address the more complex issue of simultaneously receiving communications from a swarm of probes all headed to the same target but whose launches are separated in time enough to lead to an angular spread in probes requiring a larger instantaneous field of view or *coverage*. A larger coverage results in a lower receiver sensitivity [9]. Two limiting cases are listed in Tbl.1:

- For the “swarm” case, the relatively large coverage solid angle Ω_A in Tbl.1 allows a single receive collector to capture a superposition of signals from all the probes in a swarm that are transmitting simultaneously. As illustrated in Fig.2, parallax and proper motion of the star cause this coverage to expand as the number of probes operating downlinks concurrently increases. For this reason, downlink operation for other than scientific data purposes should be kept to a minimum, and the duration of downlink operation (and hence total data volume) should also be minimized. The optimum downlink operation time is found to be about 10% of the transit time, which is 2.12 yr. With a 30-day inter-launch interval, there are 26 downlinks operating at any given time.
- For the “single” case, coverage is assumed to be limited to a single probe. That coverage will be lower bounded

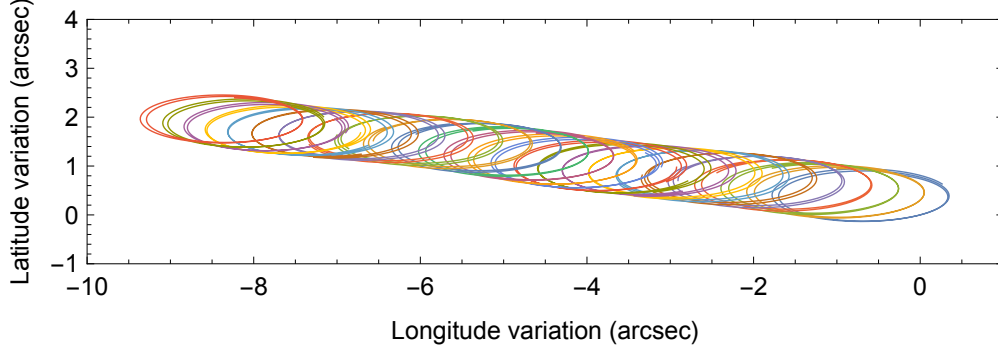


Fig. 2 Relative angle of probe trajectories as seen from a terrestrial receiver. Shown in different colors are the trajectories over 2.12 years of downlink operation for each of 26 probes launched at 30 day intervals. The oval shape for each probe’s trajectory is due to the parallax effect as the probe as viewed from different locations on the earth’s orbit. The general drift in the trajectories is due to the proper motion of the target star Proxima Centauri, which requires the launch angle of the probes to change so as to track the target.

Table 2 Performance metrics for the parameters of Tbl.1. Average transmit power scales in proportion to data rate while other metrics remain unchanged.

Parameter	Description	Units	Swarm	Single
BPP	Photon efficiency with reliable recovery of scientific data	bits/ph	10.9	
\mathcal{R}_a	Actual scientific data rate following outages	bits/s	0.43	
A_e^S	Receiver: Effective area of an aperture	cm ²	6.8	6800.
N^S	Receiver: Number of replicated apertures		5.9×10^7	2.2×10^6
$N^S \cdot A_e^S$	Receiver: Total of aperture effective areas	km ²	0.04	1.5
P_A^T	Transmitter: Average transmitted power	mW	29.4	0.8

by the pointing accuracy that can be achieved. With adaptive optics, it is assumed that a pointing accuracy of approximately 0.1 arcsec may be achievable, with the conclusion that a coverage solid angle of about 0.01 as² will ensure that the probe trajectory falls within the coverage area.

There are a number of scenarios that fall between these limiting cases. For example, the coverage could be reduced with a more rapid launch sequence interspersed with a launch holiday larger than the transmission time, thereby limiting the effect of star proper motion.

B. Receive collector decomposition

The terrestrial receiver for the downlink captures the receive optical power using an optical *collector*. A km-scale receive collector is required to achieve sufficient detected photons to allow reliable extraction of the scientific data. A single-mode diffraction-limited aperture of this size would not only be impractically large to implement, but the pointing accuracy requirement would also be impractical and the aperture would not be able to receive data from more than a single probe at a time. These issues are all overcome by decomposing the entire collector into replicated apertures as illustrated in Fig.3. To clearly distinguish parameters and metrics, variables are labeled with a “T”, “R”, or “S” respectively depending on whether they apply to the transmitter, receive collector in its entirety, or are referenced to each aperture. Thus, in Tbl.2 the effective area of each aperture, assumed to be diffraction-limited, is A_e^S , and the number of apertures is N^S . The aperture parameters govern the sky coverage Ω_A of the receiver, and also influence the SBR. A fundamental antenna theorem tells us that for uniform coverage over a solid angle Ω_A (ideally with complete rejection of all other angles) and effective area A_e^S , we must have $A_e^S \cdot \Omega_A = \lambda_0^2$ [9]. A_e^S is an area measure capturing the aperture sensitivity (ratio of detected power to incident plane-wave electromagnetic flux), and the sensitivity and coverage are thus inversely related.

A_e^S is a metric determined by the choice of parameter Ω_A . As a result each aperture is sub-meter-scale, and hence

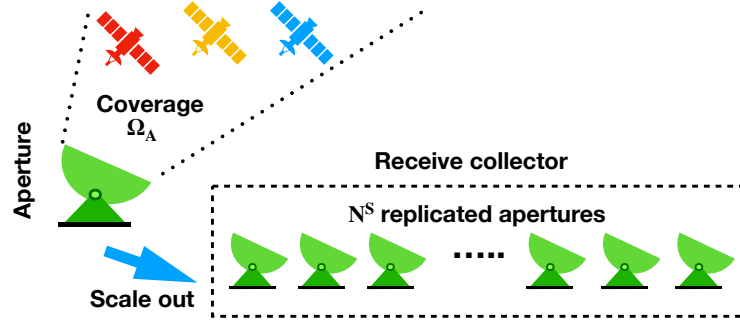


Fig. 3 The large receive collector is decomposed into a large number N^S of apertures. Each aperture controls the coverage solid angle Ω_A , and the average transmit power P_A^T is chosen to achieve the desired signal-to-background ratio SBR at the output of each aperture. The apertures operate independently and add signal photon detection events incoherently so that neither Ω_A nor SBR is affected.

achieving close to diffraction-limited performance is feasible. The photon events from the multiple apertures are added incoherently, and thus the replication of N^S apertures is a budgetary and operational (but not technological) issue.[†] Since both signal and background components add incoherently in proportion to N^S , the SBR as well as coverage are transparent to aperture replication.

The background radiation denominator of SBR at each aperture is governed by the radiation intensity, effective bandwidth W_e (in the case of noise and interference, but not dark counts), and aperture area A_e^S (only in the case of interference[‡]). Each aperture signal photon-count output is proportional to $P_A^T A_e^T / \lambda_0$, and minimizing P_A^T provides one motivation for choosing a short optical wavelength (at radio wavelengths, for example, either the transmit power or the receive collector would have to be impractically large). A second motivation is minimization of the interfering background radiation from Proxima Centauri (a red dwarf star), the spectrum of which is decreasing rapidly with shorter wavelengths in this region.

In the “swarm of probes” case in Tbl.2, the nominal number N^S of apertures is large (59 million) and their total effective area adds up to 4% of a km^2 . It is likely that this large number of apertures would be composed of sub-assemblies, each such sub-assembly containing an array of apertures manufactured as a unit. In the “single probe” case, assuming an achievable 0.1 arcsec pointing accuracy, the effective area A_e^S of each aperture is larger and the total effective area is 1.5 km^2 . In return for this tighter coverage and commensurately larger area, the average transmitted power can be considerably smaller (0.8 vs 29.4 mW) or for the same average power the data rate for the single probe can be correspondingly higher. There is thus a price to be paid for simultaneous coverage of a swarm of probes in the electrical power requirement at each probe, but a compensating payoff in a smaller total terrestrial collector area.

C. Design partitioning

The architecture of Fig.3 is dictated by the principles of antenna theory, and admits a conceptually simple functional partitioning of the design:

- The data rate \mathcal{R}_0 is determined by the rate of bursts in transmission (see §III.D.1).
- The reliability with which data is recovered at the receiver is determined by the energy associated with each burst. Since this energy requirement remains fixed, the transmitter power-area product $P_A^T A_e^T$ is proportional to \mathcal{R}_0 .
- The coverage solid angle Ω_A is determined by the effective area A_e^S of each aperture in a collector, which in turn determines the receiver sensitivity at each aperture. Thus the sensitivity of the aperture is determined by the collector coverage.
- For a fixed \mathcal{R}_0 , the SBR at each aperture necessary to achieve reliability in data recovery determines the minimum

[†] All that apertures have in common is a clock for time stamping of photon events. The relative (not absolute) clock tolerance has to be about 1 ns for the nominal design, which uses pulses with 100 ns duration at the optical detector input.

[‡] The output power of each aperture for unresolved sources of noise is proportional to A_e^S (the effective collection area) and Ω_A (the sky solid angle over which which noise enters the collector). By the antenna theorem the product of these two factors is a constant, and hence noise output power is not affected by coverage Ω_A [9].

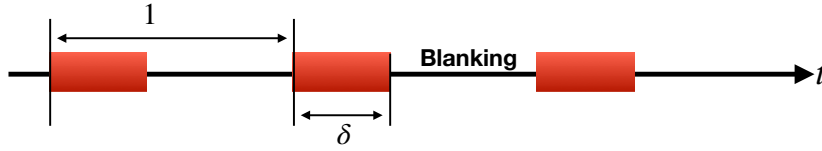


Fig. 4 An illustration of burst mode transmission. Data is transmitted in bursts with a duty cycle δ interspersed with blanking intervals during which the receiver ignores all photon events. The effective data rate during bursts is increased by factor δ^{-1} and the dark count rate is effectively multiplied by δ .

transmitter power-area product $P_A^T A_e^T$.

- Achieving a sufficient photon count K_s in each burst for reliable data recovery at the entire receive collector output determines the minimum the number N^S of apertures and thus the total receive collector effective area $N^S A_e^S$.
- It is possible to trade off total receive collector effective area $N^S A_e^S$ for lower peak and average power at the probe. This is accomplished indirectly by reducing the photon efficiency BPP. (The primary effect of reducing BPP is to increase the receive collector area, but it also reduces the required transmitted power through a reduction in the background radiation due to a smaller optical bandwidth.)

Two unavoidable and coupled constraints, the determination of aperture effective area by coverage and the accumulation of dark counts with multiple apertures, strongly influence the architecture and design. Together they eliminate some expected trade-offs such as trading a higher transmitted average power for a reduced transmit peak power (see §IV.B).

D. Optical detector and dark counts

Only very infrequent dark counts can be tolerated as an unintended side effect of the low data rate \mathcal{R}_0 and high photon efficiency BPP. We can better understand the nature of this challenge by examining the signal photon rate for the nominal values in Tbls.1 and 2. The average photon detection rate overall is $\mathcal{R}_0/\text{BPP}=0.09$ ph/s, and to achieve the SBR objective (assuming dark counts are the only source of background radiation) we must have

$$\text{SBR} = \frac{\mathcal{R}_0/\text{BPP}}{N^S \cdot \Lambda_D^S} \quad \text{or} \quad \Lambda_D^S = 1.2 \text{ ph/century} .$$

where Λ_D^S is the dark count rate referenced to one aperture. This clearly cannot be achieved in a straightforward manner. The main challenge comes from the large N^S , which results in an accumulation of dark counts when each aperture has an independent optical detector. Clearly we must find ways to mitigate a higher dark count rate.

1. Burst mode transmission

A first dark count mitigation strategy is to transmit in *burst mode*. The idea for this follows from the observation that we are not only challenged by a large N^S , but also by the small \mathcal{R}_0/BPP . Most sources of background radiation benefit from the lower bandwidth associated with a low data rate. This is also true of dark counts due to blackbody radiation in the optics and photonics, but dark counts originating in the optical detector are a notable exception. To help overcome this, as shown in Fig.4 we can artificially increase the instantaneous data transmission and signal photon rate by limiting transmission to short bursts interspersed with blanking intervals. During blanking intervals the receiver ignores all photon counts, including all sources of background radiation. This effectively reduces the dark count rate by the duty cycle δ , which is the fraction of time occupied by the data bursts. The nominal design achieves a $\delta^{-1} \sim 5300$ reduction in dark counts. Background photon detection events due to noise and interference are also reduced by factor δ , but in this case there is no net effect because an increase in optical bandwidth $W_e \sim \delta^{-1}$ admits more photons during the data bursts. This increase in optical bandwidth is beneficial in its own right since it relaxes the required selectivity of the optical bandpass filters.

2. Multiple apertures per optical detector

Even after benefiting from burst mode, the dark count rate in Tbl.1 may be beyond the capability of any current superconducting optical detectors if we maintain a one-to-one correspondence between apertures and detectors [8].

Technological progress in detectors should be feasible, including enhancing the purity of materials, radiation shielding, and techniques for eliminating some spurious photon detections. A second dark count mitigation strategy would be to share each optical detector over multiple apertures as pictured in Fig.1. The resulting reduction in the total number of optical detectors would reduce the total dark count rate. However, the incoherence of optical signals across apertures must be maintained to ensure that the coverage and SBR are not modified by this sharing. Thus optical interference among aperture optical outputs prior to detection must be avoided.

E. Optical processing

Optical processing is the manipulation of the optical signal prior to detection. To avoid optical interference between apertures, it is likely that this processing would need to be dedicated to each aperture (as opposed to each optical detector). One important function is optical bandpass filtering to limit the noise and interference reaching the detector. In the nominal design, the use of burst mode increases the optical bandwidth of the signal from $W_e=1.9$ kHz to 10 MHz, beneficially reducing the selectivity requirement for the filter. The resulting frequency selectivity is one part in 7.5×10^7 , which is within reach [10].

A major complication to the optical processing is the superposition of received signals due to multiple probes in a swarm of probes transmitting concurrently, which is called *multiplexing*.[§] Multiplexing places the additional burden on the optical processing and/or modulation coding to separate the signals from different probes before the remainder of the receiver processing. There are at least four different multiplexing techniques based on separation of signals by angle, by frequency, by time, or by code. We have not made a specific multiplexing proposal. This is a major issue affecting not only optical processing but many other aspects of the design. On initial examination time-division multiplexing seems a relatively feasible option due again to the low duty-cycle δ of burst mode. Unfortunately, synchronization of bursts between different probes is not feasible, as it would require an impractically precise clock on the probe. However, an Aloha-type protocol such as employed in ethernet [11], in which the temporal character of transmitted data bursts are deliberately randomized, may be feasible, albeit at the expense of an additional source of outages due to the infrequent random overlapping of bursts.

No matter what choices are made for aperture-sharing and multiplexing, Doppler shift will be a significant issue due to the inevitable uncertainty and tolerance in probe velocity. Because of the relativistic speed in combination with high carrier frequency, this is a significant effect. For the nominal parameterization in Tbl.1, for each $\pm 1\%$ uncertainty in probe speed there is a ± 1.6 THz Doppler shift in receive frequency. There is thus uncertainty in the receive wavelength from each probe, and different probes will have different Doppler shifts. This would be an issue to overcome in either time- or wavelength-division multiplexing. There are a combination of countermeasures that can be taken, such as launch control for precise cruise velocity, a telemetry uplink communications that operates shortly after launch for a compensating configuration of transmit wavelength, as well as possibly a need for agility and configurability in the center frequency of the receive optical bandpass filters.

IV. Probe transmitter technologies

The transmitter is constrained by the aggressive mass limitation necessary to achieve a relativistic probe speed. Thus the technological challenge is largely one of miniaturization of functions that could be readily achieved on a terrestrial laboratory bench. Where functionality is partitioned between transmitter and receiver, we obviously want to place the greater burden on the receiver. For example, the transmit aperture area A_e^T is chosen to be sub-meter-scale in Tbl.1, necessitating a km-scale receive collector in Tbl.2.

A. Electrical power supply and average power

There are three non-overlapping phases of a mission where the available electrical power will be limiting: Scientific data collection, data preparation prior to operation of the downlink (such as data compression, addition of error-correction redundancy, and interleaving), and transmission back to earth. In particular, the electrical power during transmission must be larger than the average transmit power P_A^T , with a nominal value of 30 mW in Tbl.2. As this power is directly proportional to the scientific data rate \mathcal{R}_0 , it could be reduced at the expense of reduced total data volume.

The power-area-area metric $P_A^T A_e^T \cdot N^S A_e^S$ is proportional to BPP^{-1} , and thus is moderated by achieving a high photon efficiency (BPP in bits/ph). The transmission is based on pulses with too few detected photons K_s to be recovered

[§] Even when a receive collector is dedicated to each probe there will be an additional source of interference from other probes which occupy an overlapping bandwidth.

reliably at the receiver. The design makes up for this by adding large amounts of redundancy, which allows scientific data to be recovered reliably. It thus trades off energy savings in individual pulse transmission/reception for the added power of transmitting the redundant data alongside the scientific data. This approach may seem surprising, but is theoretically necessary to approach theoretical limits on BPP [12].

Achieving a high reliability in scientific data recovery is the biggest challenge, with a typical requirement of one error on average in 1-10 megabits. That is the crucial role of ECC. If reliable data recovery is not demanded, there is no theoretical limit on the \mathcal{R}_0 that could be achieved.[¶]

B. Peak transmitted power

The nominal design is based on pulses that are narrow ($T_s=100$ ns) and sufficiently energetic to result in a meaningful number of photon detections ($K_s=0.2$) across the entire receive collector (all apertures). A crucial point is that these narrow energetic pulses are required at the receiver optical detector inputs, but commensurately narrow pulses are *not* necessarily required at the transmitter optical source. If these narrow pulses were generated in straightforward fashion by an optical source in the transmitter, the nominal peak transmit power would be large ($P_P^T=638$ kW for swarm reception and $P_P^T=17.4$ kW for single-probe reception). These values are likely not feasible with a miniaturized semiconductor laser, and further converting a continuous-electric power source into narrow pulses would be an issue given the mass limitation.

Before describing our proposal for achieving the required pulses at the detector, let's address why such energetic pulses are theoretically required at the optical detector for the purpose of achieving a large photon efficiency BPP. Avoiding a long theoretical development, this can be summarized intuitively in the following manner.

The number of individual photon detections is random, as dictated by quantum mechanics. At the design goal of BPP=10.9 bits/ph, each scientific data bit recovery is based on an average of 0.092 photon detection events. Given the quantum-mechanical randomness in photon detections, such a small number of photon detections is counter to the goal of reliable data recovery. The only way to achieve reliability is to recover multiple bits based on a commensurate large number of photon detections. Thus BPP=10.9 might actually be achieved by exchanging an average of 100 detected photons for 1090 bits, leaving room for the law of large numbers to dramatically improve the reliability in this exchange. This simultaneous recovery of 1090 bits is another way to describe the methodology of ECC. With this in mind, there are three intuitive explanations for the role of narrow pulses at the photon-counting detector:

- The most photon-conserving way to represent data is by the timing (as opposed to amplitude) of pulses, and the narrower the pulses the more data that can be represented by a single pulse in this manner.
- If we represent 1090 scientific data bits by 100 photon detection events on average as in our conceptual example, at a data rate of $\mathcal{R}=1$ bits/s this implies 100 photon detection events within 1090 sec, or 18 minutes. More significantly it implies that there must be 2^{1090} ($\sim 10^{328}$) distinguishable patterns of pulses, one pattern for each possible combination of 1090 bits. Compare this to the $\sim 10^{80}$ atoms in the visible universe. Fitting that huge number of distinctive patterns into 18 min is only possible if the pulses are themselves narrow to start with.
- All else equal, reducing the transmission to bursts interspersed with blanking intervals, though eliminating almost all dark counts, also reduces the pulse widths by δ^{-1} . This offers a direct tradeoff between dark count rates and pulse width that can be exploited depending on which technology achieves the greatest advances in the future.

The overall effect of data reliability and dark count mitigation on pulse widths can be seen in the nominal bandwidth $W_e=10$ MHz, which is seven orders of magnitude greater than the data rate. This bandwidth expansion is attributable to the use of sparse 100 ns pulses in a transmission with low duty-cycle.

1. Design parameter adjustment

The large peak powers that would be required at the transmitter to generate relatively narrow 100 ns pulses illustrate the technical difficulty and tradeoff between peak transmitted power and receiver dark count rates. Adjusting other parameters of the design can also increase pulse width T_s , thus easing the burden on the transmitter optical source. In particular, burst mode transmission offers a direct tradeoff between Λ_D^S and T_s , and hence peak power generation at the transmitter. Each order of magnitude reduction in Λ_D^S and compensatory order of magnitude increase in δ permits T_s to increase by an order of magnitude, all else equal. Reducing the coverage Ω_A will also reduce the required pulse energy,

[¶] There is some confusion on this point in the physics literature, where occasionally it is incorrectly represented that there is a theoretical limit on the data rate that can be achieved without consideration of the reliability of data recovery. In fact, absent a reliability requirement any data rate can be achieved, as illustrated in the limit of poor reliability by simply recovering data by a sequence of "random coin tosses" at the receiver.

although this comes at the expense of a larger total receive collector area and the need to replicate receivers, requiring in the limit a separate receiver for each probe in a swarm.

Reducing the photon efficiency objective must be compensated by a larger total receive collector effective area $N^S A_e^S$. One beneficial side effect of exercising this tradeoff turns out to be a reduction in transmitted average and peak power due to a resulting decrease in total background radiation due to a decrease in optical bandwidth. Thus reducing photon efficiency in the context of burst mode and the collector architecture of Fig.3 implicitly exchanges larger total collector area for smaller transmit average and peak power.

Our approach in Tbl.1 is to choose a signal level larger than the background level ($SBR > 1$). It is also feasible to operate with $SBR < 1$, although the theoretical photon efficiency falls off rapidly as SBR decreases in this regime. While this would allow for greater dark count rates, all else equal, it would have other negative consequences.

2. Employing optical interference

Optical interference can be used in place of emitting high powers directly from an optical source. A straightforward example of this is the ganging of multiple semiconductor lasers in the transmitter with an optical combiner. Unfortunately this is expected to be inconsistent with the low-mass objective.

Pulse compression technology, often used to generate narrow laser pulses, converts a longer-duration waveform, albeit a waveform with the same bandwidth as the narrow pulses, into narrow pulses by utilizing wavelength-dependent group delays to align shorter- and longer-frequency components in time. This would have to be done in the optical realm, and could presumably be accomplished in either transmitter or (more interestingly) receiver. Typical arrangements utilize pairs of diffraction gratings or prisms to provide the wavelength-dependent variable group delays. While this technique is often used to generate picosec pulses, it does not appear to be feasible for the microsec-scale pulses in our application due to the microsec-scale delays that would be required and the resulting large physical scale (light travels a meter in ~ 3 nanosec in a vacuum). Burst mode offers the freedom to reduce pulse widths arbitrarily, bringing us into the feasible range of pulse compression, but at the expense of a commensurately larger peak-power requirement.

3. Changing the modulation format

The model used to quantify the metrics in Tbl.2 assumes a modulation code which operates at a single wavelength and represents scientific data by the timing of narrow pulses in transmit and received power. This is only one of a class of theoretically equivalent modulation codes based on orthogonal codewords in the space of temporal and wavelength modes.

A second approach is to represent data by different wavelengths rather than different times. While this requires a wavelength-agile optical source at the transmitter, a significant advantage is a constant transmit power. However, the complexity of this frequency-shift keying receiver is significantly increased, as a high spectral resolution would be required with optical detectors replicated at the distinctive wavelengths. Such a proliferation of detectors would appear to multiply the dark count rates accordingly.

A third approach to modulation is code-division keying, in which a set of orthogonal codes (rather than times or wavelengths) are used [13]. These codes can also be designed with constant power over the codeword, and they are distinguished at the receiver by filters matched to each codeword utilizing again optical interference. Again an entire bank of optical detectors is required, one detector for each matched filter, and there is therefore the expectation that dark counts are multiplied.

V. Conclusions

There are a considerable number of obstacles to achieving the downlink objectives with a focus on a large multiple probe swarm. We have outlined the most troublesome ones identified to date, suggesting considerable need and opportunity for R&D efforts directed at overcoming these obstacles. Readers with relevant expertise are encouraged to tackle these challenges. While there is some opportunity for architectural and system innovations, the major need is early feasibility demonstration of novel photonics technology and architectures for high-peak power optical sources, very frequency-selective optical filters (including delay equalization and band limitation) and optical detectors with very low dark count rates. Also required is an early and credible proposal for, and choice of, a modulation coding and multi-probe multiplexing strategy.

Acknowledgments

PML gratefully acknowledges funding from NASA NIAC NNX15AL91G and NASA NIAC NNX16AL32G for the NASA Starlight program and the NASA California Space Grant NASA NNX10AT93H, a generous gift from the Emmett and Gladys W. Technology Fund, as well as support from the Breakthrough Foundation for its StarShot program. More details on the NASA Starlight program can be found at www.deepspace.ucsb.edu/Starlight.

References

- [1] Lubin, P., “A Roadmap to Interstellar Flight,” *Jour. British Interplanetary Soc.*, Vol. 69, 2016, pp. 40–72.
- [2] Parkin, K., “The Breakthrough Starshot system model,” *Acta Astronautica*, Vol. 152, 2018. <https://doi.org/10.1016/j.actaastro.2018.08.035>.
- [3] Parkin, K., “A StarShot Communication Downlink,” *arXiv preprint arXiv:2005.08940*, 2019.
- [4] Messerschmitt, D. G., P.Lubin, and Morrison, I., “Challenges in Scientific Data Communication from Low-Mass Interstellar Probe,” *arXiv preprint arXiv:1801.07778*, 2020.
- [5] Messerschmitt, D., Lubin, P., and Morrison, I., “Technological Challenges in Low-mass Interstellar Probe Communication,” *Tennessee Valley Interstellar Symposium*, Wichita, KN, 2019.
- [6] Messerschmitt, D., “BPPM modeling software,” , 2020. <https://doi.org/10.5281/zenodo.3831502>, URL <https://doi.org/10.5281/zenodo.3831502>.
- [7] Farr, W. H., Choi, J. M., and Moision, B., “13 bits per incident photon optical communications demonstration,” *Free-Space Laser Communication and Atmospheric Propagation XXV*, Vol. 8610, International Society for Optics and Photonics, 2013, p. 861006. <https://doi.org/10.1117/12.2007000>.
- [8] Shibata, H., Shimizu, K., Takesue, H., and Tokura, Y., “Ultimate low system dark-count rate for superconducting nanowire single-photon detector,” *Optics Letters*, Vol. 40, No. 14, 2015, pp. 3428–3431. <https://doi.org/10.1364/OL.40.003428>.
- [9] Burke, B., and Graham-Smith, F., *An introduction to radio astronomy*, Cambridge University Press, 2009. <https://doi.org/10.1017/CBO9780511801310>.
- [10] Shtyrkova, K., Gaschits, I., and Caplan, D., “Narrowband optical filtering for background-limited photon-counting free-space optical communications,” *Free-Space Laser Communications XXXI*, Vol. 10910, International Society for Optics and Photonics, 2019, p. 109100F.
- [11] Abramson, N., “Multiple access in wireless digital networks,” *Proceedings of the IEEE*, Vol. 82, No. 9, 1994, pp. 1360–1370.
- [12] Butman, S., Katz, J., and Lesh, J., “Bandwidth limitations on noiseless optical channel capacity,” *IEEE Transactions on Communications*, Vol. 30, No. 5, 1982, pp. 1262–1264. <https://doi.org/10.1109/TCOM.1982.1095577>.
- [13] Banaszek, K., and Jachura, M., “Structured optical receivers for efficient deep-space communication,” *2017 IEEE International Conference on Space Optical Systems and Applications (ICSOS)*, IEEE, 2017, pp. 34–37. <https://doi.org/10.1109/ICSOS.2017.8357208>.